Origin and pathways of Winter Intermediate Water in the Northwestern Mediterranean Sea using observations and numerical simulation

Mélanie Juza,[1] Lionel Renault,[1,2] Simon Ruiz,[3] and Joaquin Tintoré[1,3]

[1] The study of water masses worldwide (their formation, spreading, mixing, and impact on general circulation) is essential for a better understanding of the ocean circulation and variability. In this paper, the formation and main pathways of Winter Intermediate Water (WIW) in the Northwestern Mediterranean Sea (NWMED) are investigated during the winter-spring 2011 using observations and numerical simulation. The main results show that the WIW, formed along the continental shelves of the Gulf of Lion and Balearic Sea, circulates southward following five preferential pathways depending on the WIW formation site location and the oceanic conditions. WIW joins the northeastern part of the Balearic Sea, or flows along the continental shelves until joining the Balearic Current (maximum of 0.33 Sv in early-April) or further south until the Ibiza Channel entrance. Two additional trajectories, contributing to water mass exchanges with the southern part of the Western Mediterranean Sea, bring the WIW through the Ibiza and Mallorca Channels (maxima of 0.26 Sv in late-March and 0.1 Sv in early-April, respectively). The circulation of WIW over the NWMED at 50–200 m depth, its mixing and spreading over the Western Mediterranean Sea (reaching the south of the Balearic Islands, the Algero-Provencal basin, the Ligurian and the Alboran Seas) suggest that the WIW may have an impact on the ocean circulation by eddy blocking effect, exchange of water masses between north and south subbasins of Western Mediterranean Sea through the Ibiza Channel or modification of the ocean stratification.

1. Introduction

[2] The Northwestern Mediterranean Sea (NWMED) comprises the Gulf of Lion and the Balearic Sea. Its general surface circulation is characterized by the presence of two quasi-permanent currents, the Northern Current (NC) and the Balearic Current (BC), and their associated fronts (Figure 1a). The Catalan Front is a shelf/slope front that separates the "old" Atlantic Water (AW) in the center of the Balearic Sea from the less dense water, transported by the NC, on the shelf [*Font et al.*, 1988]. The NC flows southward along the continental slope reaching and going through the Ibiza Channel or retroflecting cyclonically over the northern slopes of the Balearic Islands to form the BC; this latter is also fed by the inflow of more recent warm and fresh AW arriving from south through the Mallorca and Ibiza Channels [e.g., *Font et al.*, 1988; *Pinot et al.*, 1995, 2002; *Pinot and Ganachaud*, 1999]. The Balearic Front separates the saltier "old" AW in the central part of the Balearic Sea from the less dense water transported by the BC [*Font et al.*, 1988; *La Violette et al.*, 1990; *Bouffard et al.*, 2010]. Observations have shown that both currents have a marked seasonal variability [*Béthoux*, 1980; *Font et al.*, 1988; *Pinot et al.*, 2002]. Higher transports in the NC are found in winter (1.5–2 Sv) than in summer (1 Sv), while the opposite is found in the BC (0.3 Sv in winter, 0.6 Sv in summer). In addition to the basin-scale circulation, several studies have shown significant mesoscale structures such as eddies, filaments, and shelf-slope flow modifications [*Font*, 1990; *La Violette et al.*, 1990; *Pinot et al.*, 2002; *Bouffard et al.*, 2010, 2012]. The NWMED is also characterized by intense Mistral, Tramontane, and Cierzo winds episodes in winter [*Jansá*, 1987; *Millot*, 1999]. These winds induce intense heat air-sea exchanges [*Flamant*, 2003; *Renault et al.*, 2012] and sea surface cooling [*Millot*, 1999; *Estournel et al.*, 2003].

[3] The NWMED is a four-layer system, comprising different water masses [*La Violette*, 1994; *Send et al.*, 1999; *Robinson et al.*, 2001], originating from the Atlantic Ocean and the Eastern Mediterranean Sea or formed in the

[1]SOCIB, Palma de Mallorca, Spain.
[2]UCLA, Atmospheric and Oceanic Sciences, Los Angeles, California, USA.
[3]IMEDEA (UIB-CSIC), Esporles, Islas Baleares, Spain.

Corresponding author: M. Juza, SOCIB, Parc Bit, Naorte, Bloc A 2 p. pta. 3, Palma de Mallorca ES-07121, Spain. (mjuza@socib.es)
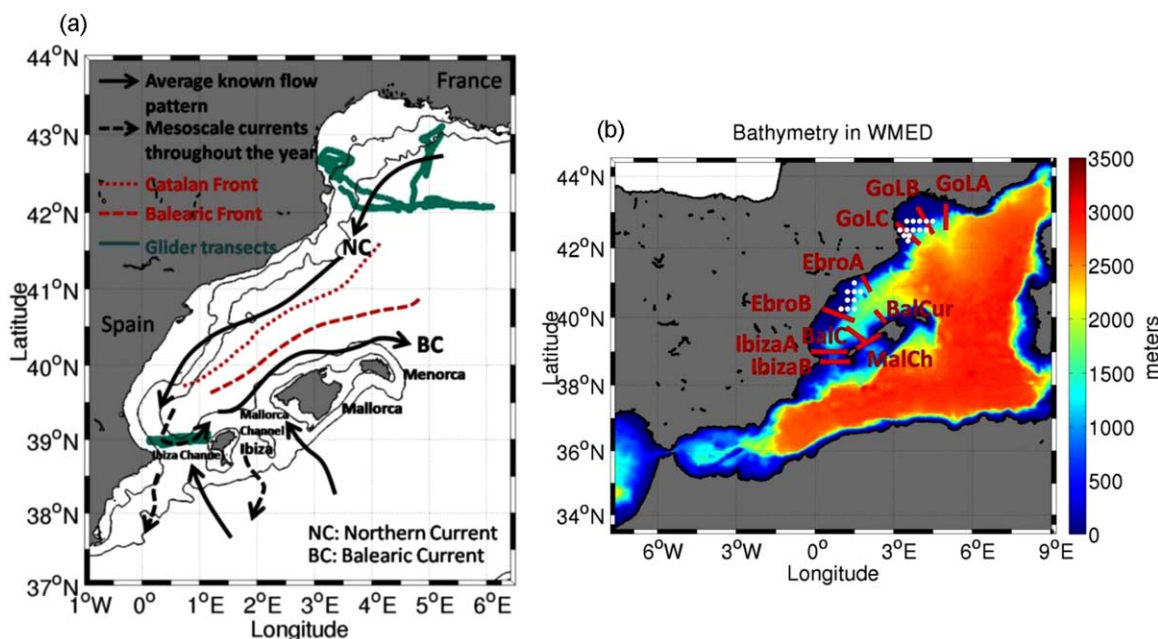
Figure 1. (a) General surface circulation in the NWMED; glider transects in Gulf of Lion (March 2011) and across the Ibiza Channel (January–June 2011). (b) WMOP model configuration. Color bar indicates model bathymetry. The sections (red lines) and the start positions of Lagrangian particles (white points), used in section 4, are superimposed.

NWMED. In the upper 150 m layer, the AW gets into the Mediterranean Sea at the surface through the Gibraltar Strait and, circulating in the Mediterranean Sea, becomes saltier (from 36.5 at Gibraltar to 38.0–38.3 in the NWMED) due to the air-sea interactions and mixing [*Millot*, 1999]. Below the surface layer, the Levantine Intermediate Water (LIW), formed in the Eastern Mediterranean Sea, gets into the Western Mediterranean Sea (WMED) through the Sicily Channel, probably mixed with the Cretan Intermediate Water [*Millot*, 2013]. The LIW is characterized by temperature (T) and salinity (S) maxima (14–13.2°C and 38.7–38.5, respectively) generally found at 300–400 m depth [*Astraldi et al.*, 1999; *Millot*, 1999]. Besides, two water masses are formed in the NWMED. The Winter Intermediate Water (WIW) is formed under severe winter conditions, predominantly along the continental shelf in the Gulf of Lion and the Balearic Sea (despite the influence of low salinities of continental origin) through winter convection of the AW [*Salat and Font*, 1987; *Millot*, 1999; *Pinot and Ganachaud*, 1999]. The WIW is identifiable by a minimum of T in the intermediate layer between the AW in the surface and the denser LIW. This water mass is characterized by T of 11.5–13°C and S of 37.7–38.3 [*López-Jurado et al.*, 1995; *Vargas-Yáñez et al.*, 2012]. The WIW circulates in the WMED, transported southward through mode water eddies advected by the NC [*Pinot et al.*, 2002]. The WIW is not formed every year and interannual variability of its quantity has been observed in the Balearic Sea [*Pinot et al.*, 2002; *Monserrat et al.*, 2008]. The presence of WIW in the Balearic Sea can induce eddy formation and influences the circulation through the Balearic Channels [*López-Jurado et al.*, 1995; *Pinot et al.*, 1995, 2002; *Astraldi et al.*, 1999; *Pinot and Ganachaud*, 1999; *Amores et al.*, 2013]. Although this

study focuses on the NWMED (Gulf of Lion and Balearic Sea), note that WIW can be formed in the Ligurian Sea [*Sparnocchia et al.*, 1995; *Gasparini et al.*,1999] and likely in the western Tyrrhenian Sea [*Ben Ismail et al.*, 2012]. Under severe winter conditions, the Gulf of Lion is also the place where deep convection and formation of Western Mediterranean Deep Water (WMDW) may occur [*Mertens and Schott*, 1998; *Salat et al.*, 2010]. The WMDW production has been possibly influenced by the Eastern Mediterranean Transient which favored the passage of highly saline intermediate masses through the Strait of Sicily toward the WMED [*Gasparini et al.*, 2005; *Schroeder et al.*, 2008; *Herrmann et al.*, 2010]. The WMDW occupies the deep layer, generally greater than 1500 m [*Millot and Taupier-Letage*, 2005].

[4] The formation of WMDW has been largely studied, whereas the origin of WIW is more poorly described. Most of studies about the WIW investigate its formation locally (in the Ligurian Sea [*Gasparini et al.*, 1999], in the Gulf of Lion [*Dufau-Julliand et al.*, 2004], in the Balearic Sea [*Vargas-Yáñez et al.*, 2012], and in the Channel of Sicily [*Ben Ismail et al.*, 2012]), or its presence and its impact on regional dynamics in the NWMED using observations [*López-Jurado et al.*, 1995; *Pinot et al.*, 1995; *Heslop et al.*, 2012] or both observations and numerical simulations [*Pinot and Ganachaud*, 1999; *Pinot et al.*, 2002]; but these latter studies are limited to subbasins, in particular the region of the Balearic Channels. *Heslop et al.* [2012], using glider data, show the presence of WIW in the Ibiza Channel during the winter 2011. From the available surface data (provided by oceanographic buoys and satellite), they suggest this water mass may likely originate from the Gulf of Lion or the Balearic Sea. Nevertheless, due to the lack of data, *Heslop et al.* [2012] were not able to determine

when and where WIW is formed. The use of a high resolution oceanic numerical simulation could overcome this issue and complement the data to understand the origin and the pathways of the WIW in the NWMED during such period. In this study, using both observations and oceanic numerical simulation, the main objective is to document the principal pathways of WIW in the NWMED during winter-spring 2011. In this sense, the present work is an extension of the former studies by e.g., *Pinot and Ganachaud* [1999], *Pinot et al*. [2002], and *Heslop et al*. [2012].

[5] The paper is organized as follows: the observations, the numerical simulation, and the methodology are described in section 2. Section 3 presents the atmospheric conditions and an overview of the scene from the observations. Then, the simulation is evaluated with respect to the observations. In section 4, the simulation is used to investigate the formation and pathways of WIW in the NWMED in winter-spring 2011. Finally, conclusions are given in section 5.

2. Data Sets and Methodology

2.1. In Situ Observations

[6] The ENACT-ENSEMBLES EN3_v2a database [*Ingleby and Huddleston*, 2007] provides in situ T/S profiles collected worldwide using bathythermographs, Argo floats, and hydrographic transects (CTDs). All suspicious (flagged) data were rejected for this study. Although the spatial and temporal coverage remains poorly sampled in the WMED, many T/S profiles have been collected in March 2011 during three glider deployments in the Gulf of Lion (Figure 1a).

[7] Data from IMEDEA gliders operated by SOCIB in the Ibiza Channel semicontinuous endurance line (Figure 1a) from January to June 2011 [*Heslop et al*., 2012; *Tintoré et al*., 2013] are also used to monitor the presence of WIW through the Ibiza Channel. A Slocum deep glider provided high-resolution hydrographic data between depths of 20 m and 950 m with a horizontal resolution of 2 km approximately. The glider data processing includes the thermal lag correction [*Garau et al*., 2011] for unpumped CTD sensors installed on Slocum gliders.

2.2. Models Description

[8] The oceanic model used is the Regional Ocean Modeling System (ROMS) [*Shchepetkin and McWilliams*, 2005], a 3D free-surface, sigma coordinate, split-explicit equation model with Boussinesq and hydrostatic approximations. The model domain extends from 7.8°W to 9.2°E and from 33.4°N to 44.5°N (Figure 1b). The vertical discretization considers 32 sigma levels, and the horizontal grid is 681 × 574 points with a resolution of 2.1 km (1/40°), which allows the representation of mesoscale structures in this region where the first internal deformation radius is around 10–15 km [*Send et al*., 1999]. The bathymetry is derived from 1′ topography database [*Smith and Sandwell*, 1997]. The simulation is nested and initialized from the Mercator PSY2V4R3 simulation [*Lellouche et al*., 2013] on 1 February 2011 and lasts 5 months. Due to the lack of data assimilation in the ocean model, a short spin-up (15 days) is used to avoid too much drift of the ocean model from observed conditions. Thus, the simulation will be used from the 15 February 2011. At the boundaries, mixed active-passive conditions are used [*Marchesiello et al*.,

2001] with forcing data from the Mercator PSY2V4R3 simulation, which has a 1 day temporal resolution and a 1/12° spatial resolution with 50 vertical zeta levels. Our model outputs are daily means. A similar configuration of the atmospheric model Weather Research and Forecasting (WRF) [*Skamarock et al*., 2008], described and used in *Renault et al*. [2011] and *Ruiz et al*. [2012], forces ROMS using bulk formulae [*Fairall et al*., 2003] to compute turbulent heat and momentum fluxes. The WRF simulation is performed using a two-way nesting technique, and its initial and boundary conditions are provided by the NCEP FNL analysis which has a 1° spatial resolution and a 6 h temporal resolution (http://dss.ucar.edu/datasets/ds083.2).

[9] Note this ROMS configuration has a finer resolution that the PSY2V4R3 simulation allowing a better reproduction of (sub-)mesoscale features. Additionally, in this simulation, the WIW will be formed without data assimilation.

2.3. Methodology

[10] First, the observations are used to highlight the presence of WIW over the NWMED in winter 2011. Then, the simulation outputs are systematically interpolated at the observed space-time positions for comparison with observations. In this way, the capacity of the simulation to reproduce the observed water masses is evaluated. Finally, when investigating the WIW pathways, the fully sampled simulation is used to fill the observations subsampling. Note that since this paper focuses on both formation and spreading of WIW over the NWMED in a realistic scenario, the period of study is from mid-February to the end of June 2011 because observational data are available both in the Gulf of Lion and the Ibiza Channel to show the presence of WIW and assess the simulation, and to investigate the WIW propagation in winter-spring 2011.

[11] The Lagrangian tool implemented in ROMS (www.myroms.org) was used to track the WIW pathways. The particle location at each time is determined using the 4th order Milne-predictor/Hamming-corrector numerical integration scheme [*Hamming*, 1959]. In the simulation, during the strong wind event occurring from 27 February to 5 March 2011, square networks of 16 particles space by 0.03° (1.2–1.6 km) were daily released at 20, 50, 100, and 200 m depths at each release sites (Figure 1b). They are located in the two main areas of WIW formation, in the Gulf of Lion and the Ebro Delta region. In total, almost 10,000 particles have been launched. Once released, the particles acted as 3D Lagrangian particles embedded in the circulation flow fields and were tracked for all the simulation times. In this paper, only particles with WIW characteristics ($11.5 < T < 13°C$, $37.7 < S < 38.3$) are examined.

[12] To support the determination of WIW pathways, transports are estimated in the simulation through ten key sections (Figure 1b) for water with WIW characteristics from 15 February to 30 June 2011. The sections have been selected in the areas of WIW formation (Gulf of Lion: *GoLA*, *GoLB*, *GoLC*; Balearic Sea near the Ebro Delta: *EbroA*, *EbroB*) and the possible WIW pathways (Ibiza Channel: *IbizaA*, *IbizaB*; Balearic Current: *BalC*, *BalCur*; Mallorca Channel: *MalCh*), capturing the maximum of WIW transport through the associated transect. Note that the sections *GoLC* and *IbizaA* correspond to the glider sections in March and February–June 2011, respectively. The inflow (outflow) transport is
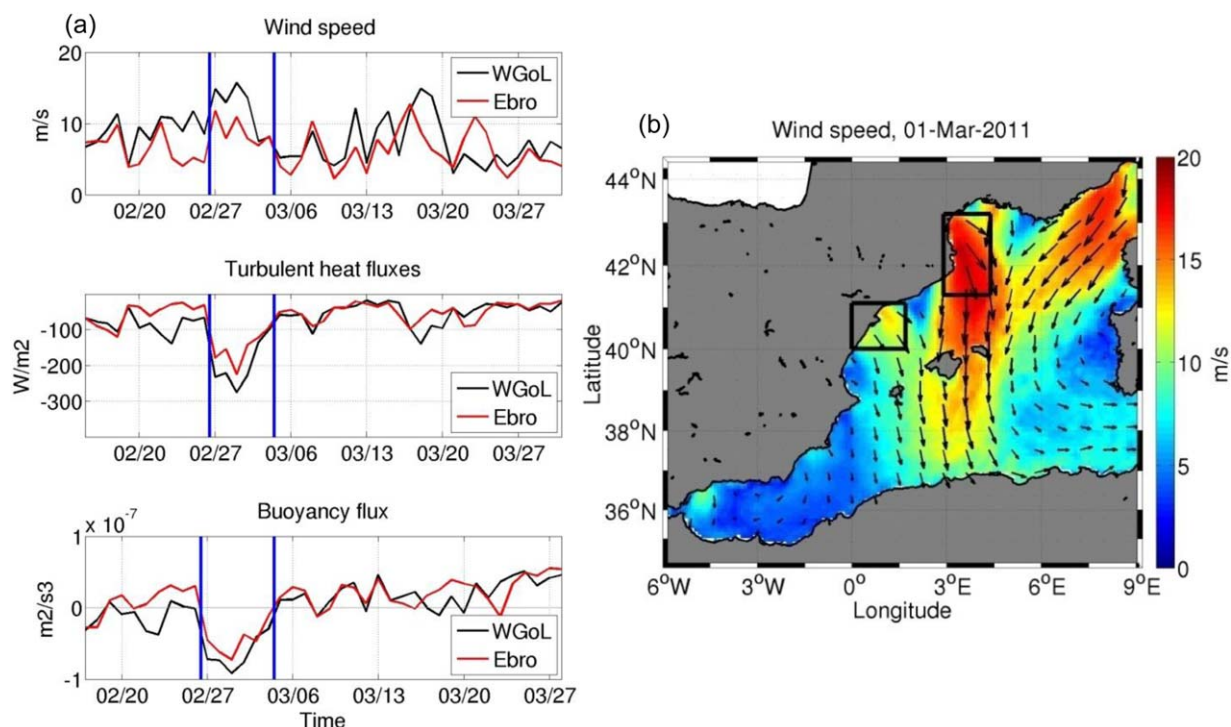
Figure 2. (a) Time series of the (top) simulated wind speed, (middle) turbulent heat fluxes, and (bottom) buoyancy flux from 15 February to 31 March 2011 in the Western Gulf of Lion (WGoL) and the Ebro Delta region (Ebro). (b) Wind speed the 1 March 2011 in the WMED.

associated to positive (negative) values indicating northward/eastward (southward/westward) direction.

3. Overview of the Event Period

3.1. Atmospheric Conditions

[13] Figure 2a shows the WRF simulated 10 m wind speed time series averaged over the Western Gulf of Lion (WGoL) and the Ebro Delta region (Ebro) (see boxes in Figure 2b) from 15 February to 31 March 2011. Both regions experience some intense wind episodes. In particular, as illustrated in Figure 2b, the Gulf of Lion and Balearic Sea are characterized by an intensification of the Tramontane and Cierzo winds the 1 March 2011 inducing wind gusts reaching up to 20 m/s. Between the 27 February and 5 March 2011 (Figure 2a), the wind intensification over WGoL and Ebro induces strong air-sea interactions that cause significant heat loss by turbulent fluxes (up to -275 W/m^2 and -225 W/m^2, respectively, the 1 March 2011) and then a decrease of the buoyancy flux associated with the heat flux (up to -0.92×10^{-7}m^2/s^3 and -0.73×10^{-7}m^2/s^3, respectively). Since the WIW is formed by convection when heat losses in winter are important but not large enough to produce deep water [*Sparnocchia et al.*, 1995; *Gasparini et al.*, 1999; *Pinot et al.*, 2002], the atmospheric conditions could induce WIW formation over this period.

3.2. Observed and Simulated Water Masses

[14] The observations available in the Gulf of Lion confirm the presence of WIW and typical characteristics of water masses structures [*Millot*, 1999] during this period (Figure 3a): the AW at the surface with T > 13°C, the LIW

with T > 13°C and maxima of S, the WIW with T < 13°C and 37.7 < S < 38.3, and the WMDW with T < 13°C and S > 38.44 in the deeper layer. Although slight T/S biases in the simulation are found (median value of 0.006°C/0.01, respectively), the simulated T/S diagram in the Gulf of Lion in March 2011 (Figure 3b) indicates the simulation is able to reproduce the observed water masses characteristics. More precisely, Figures 3c and 3d show the vertical sections of temperature and salinity from observations and simulation, respectively, in the western coastal area of the Gulf of Lion (Figure 1a), where WIW is found in March 2011. They show that the observed WIW occupies the upper 300 m of the continental shelf. Despite temperature and salinity biases, both formation of WIW by surface cooling of AW and WIW layer are well reproduced by the simulation.

[15] In the Ibiza Channel, as highlighted by *Heslop et al.* [2012] and in Figure 4a, the observations reveal the presence of WIW from February to May 2011. Despite slight T/S median biases (0.02°C/0.04, respectively), the simulation reproduces relatively well the observed water masses across the Ibiza Channel (Figure 4b). A closer inspection of all the vertical sections of observed T and S (not shown) indicates the WIW is mainly present in the Ibiza Channel in March–April 2011 at 50–200 m depth (Figure 4c) and is well represented in the simulation (Figure 4d).

4. Origin and Pathways of Winter Intermediate Water

4.1. Spatial Trajectories

[16] Figure 5 shows the Lagrangian trajectories of the simulated particles (section 2.3) having the WIW characteristics. In
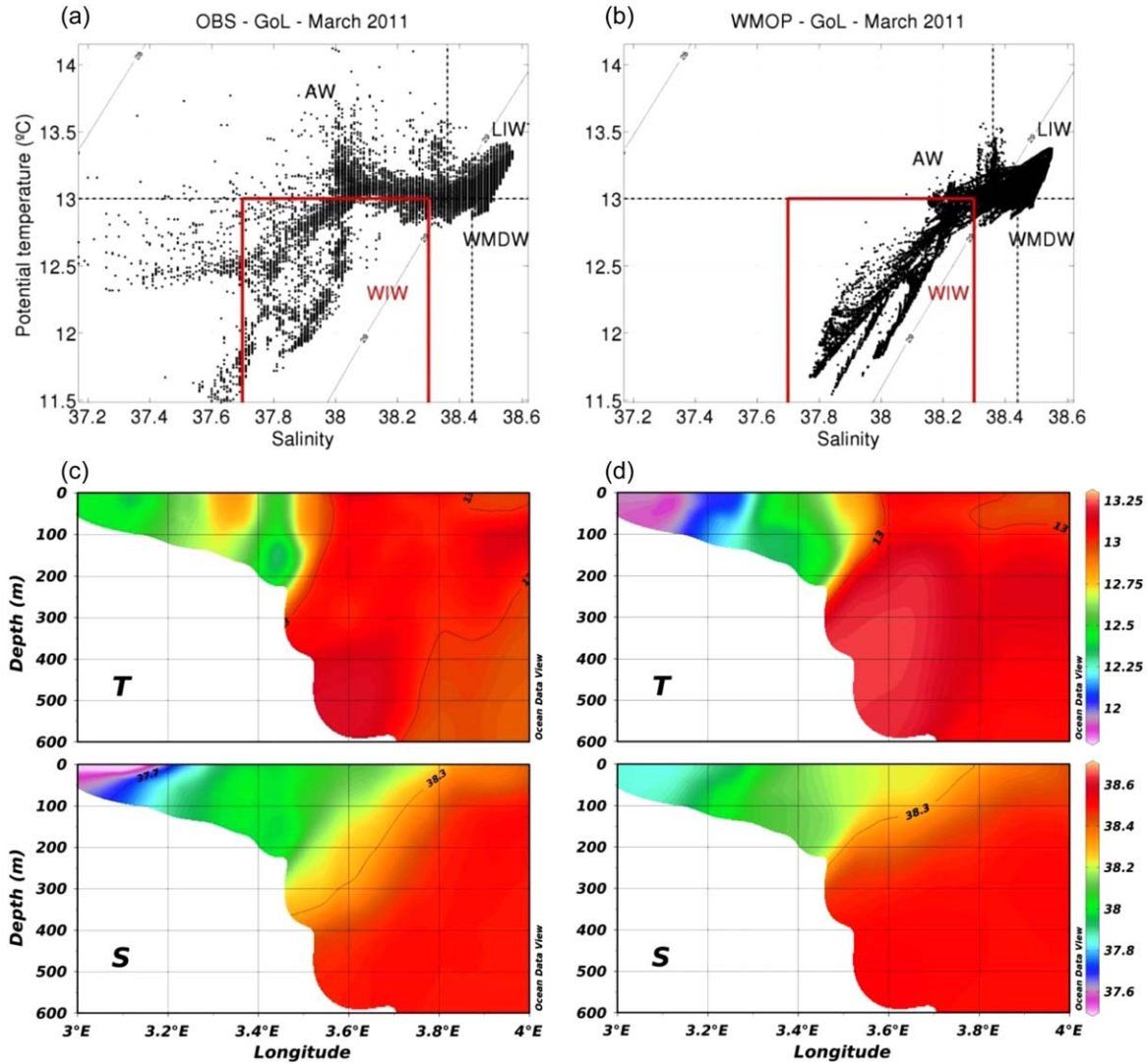
Figure 3. (a and b) T/S diagrams of the observations and the simulation (interpolated at the observed space-time positions) in the Gulf of Lion in March 2011. Boxes delimit the temperature and salinity ranges of the water masses. Associated vertical sections of temperature and salinity from (c) observations and (d) simulation in the western part of the coastal area where WIW is present.

good agreement with the literature, most of the simulated WIW is formed along the continental shelves of Gulf of Lion and Balearic Sea, and circulates southward in the Balearic Sea (Figures 5a and 5c) reaching 100–200 m depth (Figures 5b and 5d).

[17] Some particles remain in their formation region losing their WIW properties. Excluding them, the main pathways from the Gulf of Lion and the Ebro Delta region (P_G and P_E, respectively) can be depicted from Figure 5. From the Gulf of Lion (Figures 5a and 5b), the first one (P_G^1) follows the NC along the coast until 2.2°E and 41.2°N, and then brings WIW (43%) to the North of Mallorca in the upper 80 m in less than 20 days, that finally loses its characteristics (mid-March). P_G^1 is associated to (sub-)mesoscale features as revealed by the simulated currents averaged in the upper 200 m and the sea surface temperature in mid-March (e.g., the 17 March 2011, Figure 6). The second trajectory (P_G^2) leading WIW (24%) follows the NC

along the Catalan coast, that then deflects at 0.7–1.2°E and 39.2–39.6°N after 30–40 days in early-April (see e.g., the currents on the 7 April 2011, Figure 6), and then joins the BC at about 100 m depth. As indicated by the simulated currents in the upper 200 m and the sea surface temperature on the 7 April 2011 (Figure 6), this trajectory interacts with an entrance of warmer AW through the Ibiza Channel. The third and last pathway from the Gulf of Lion (P_G^3) is related to an intensification and a deflection further south of NC (see e.g., the 23 April 2011, Figure 6). It brings WIW (33%) along the Peninsula coast until reaching the Ibiza Channel at 120–160 m depth where particles bifurcate eastward after 45 days (mid-April) or stay at the entrance of the Ibiza Channel losing their WIW properties after 60 days (late-May). From the Ebro Delta (Figures 5c and 5d), the first trajectory P_E^1 (13%) joins P_G^1 at the North of Mallorca. The second one (P_E^2, 18%) circulates southward without going along the continental shelves and follows the NC
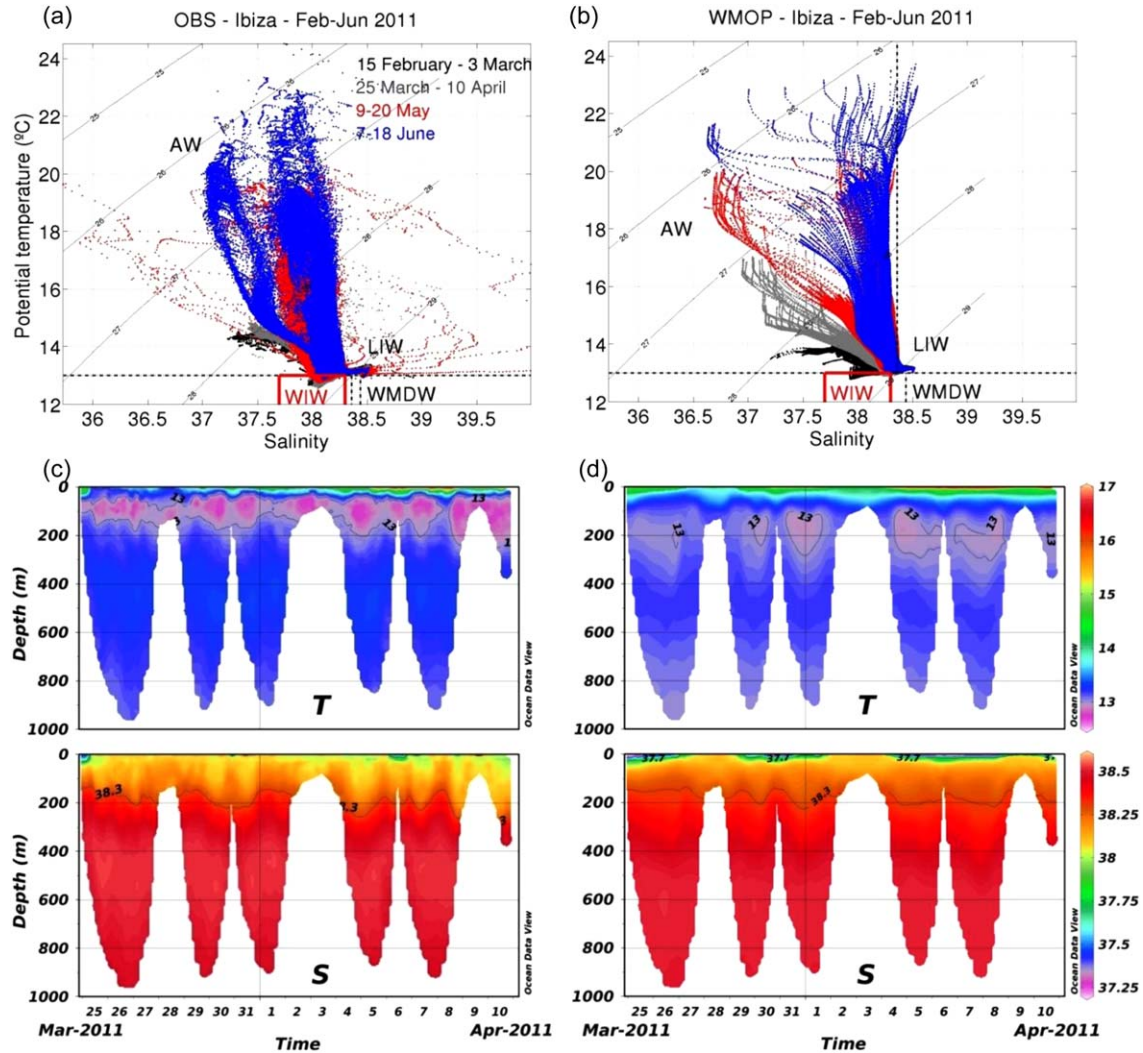
Figure 4. (a and b) T/S diagrams of the observations and the simulation (interpolated at the observed space-time positions) in the Ibiza Channel in February–June 2011. As in Figures 3a and 3b, water masses are indicated. Vertical sections of temperature and salinity from (c) observations and (d) simulation collected during the three returns in the Ibiza Channel from 25 March to 10 April 2011 when most of WIW are present in the observations.

going through the Ibiza Channel at 70–180 m depth after 20–25 days in mid-to-late March (see e.g., the 20 March 2011, Figure 6). The third and fourth pathways (P_E^3, 40% and P_E^4, 27%) follow in space and time P_G^2 and P_G^3, respectively. The last trajectory (P_E^5, 2%), going through the Mallorca Channel at 120–180 m depth after 40 days (early-April), is marginal.

[18] The WIW, formed in the Gulf of Lion and the Ebro Delta region from 27 February to 5 March 2011, circulates in the Balearic Sea (Figure 5e). Some of them (20% of those formed in the Ebro Delta region) flow out of the basin through the Balearic Channels. Figure 7 shows the spatial evolution of WIW particles that have finally lost their temperature and salinity properties after dilution with surrounding waters. The two thirds of WIW particles formed in the Gulf of Lion and the Ebro Delta region are mixed with other water masses after 20–50 days and 10–35 days, respectively (not shown). After 70 days, all of WIW particles have changed properties. This illustrates the mixing

(since the temperature and salinity minimum is diluted) and the spreading of these particles over the WMED, reaching the southern part of the Balearic Islands, the Algero-Provencal basin, the Ligurian Sea, and the Alboran Sea at the end of June 2011, and suggests that the WIW may likely have an impact on the general circulation. Indeed, the WIW formation and spreading may induce mesoscale eddies [*Amores et al.*, 2013] which influence the exchanges between the different subbasins of WMED and the basin-scale flow (e.g., eddy blocking effect in the north of the Ibiza Channel [*Pinot et al.*, 1995, 2002; *Pinot and Gana-chaud*, 1999] or contribution to exchanges between north and south subbasins of WMED by WIW eddy transport [*Allen et al.*, 2008]). Additionally, the WIW is probably a major component of the Mediterranean outflow at Gibraltar [*Fuda et al.*, 2000; *Millot*, 2009, 2013]. Finally, the mixing of WIW with surrounding water masses changes the hydro-graphic properties and the ocean stratification that may influence the ocean circulation.
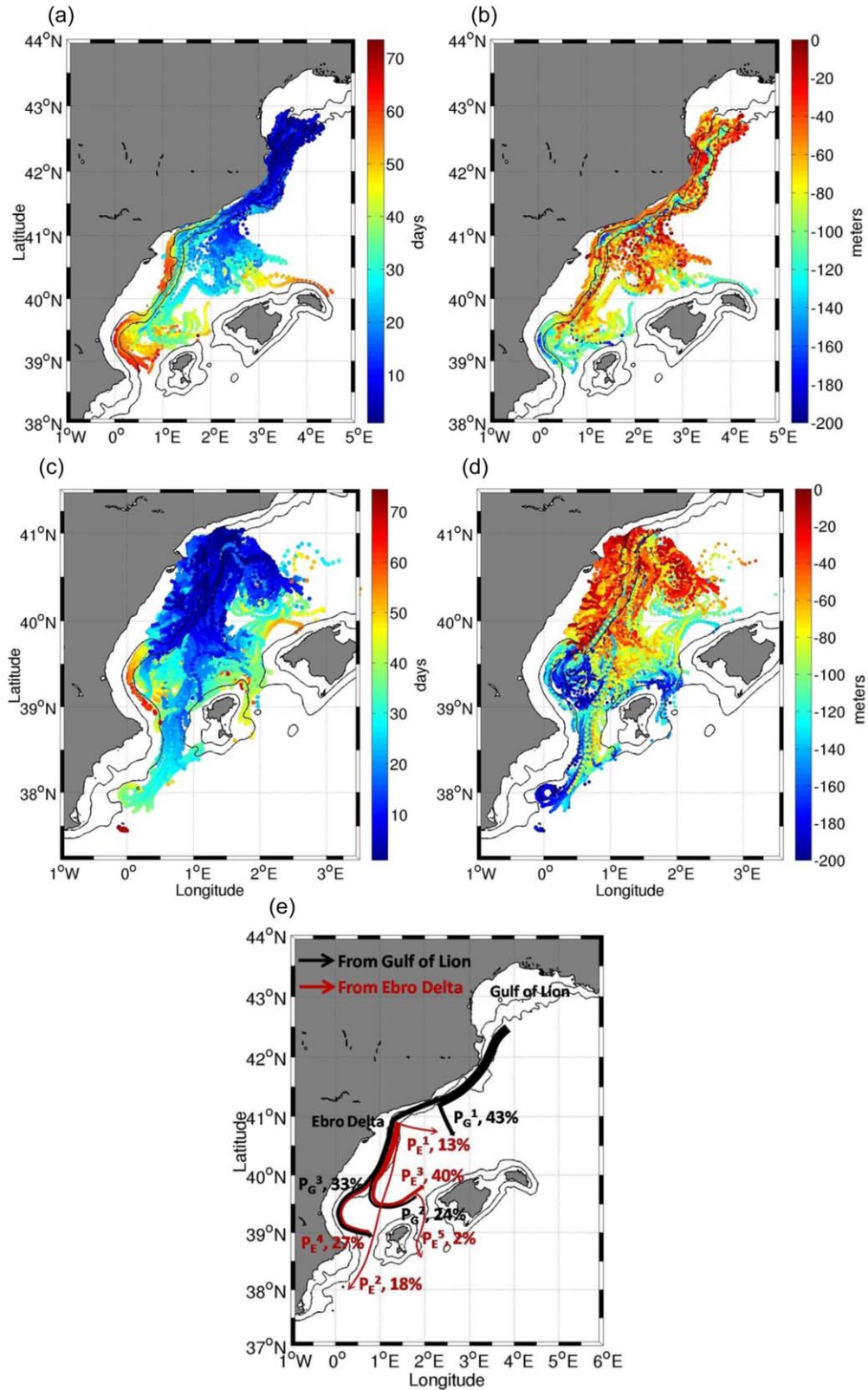
Figure 5. (a and b) Lagrangian trajectories of WIW particles from the Gulf of Lion and (c and d) the Ebro Delta region with daily starts between 27 February and 5 March 2011. Color scale indicates (a and c) time in days or (b and d) depth in meters. Only one of four trajectories is shown here for clarity. (e) Scheme of main WIW pathways.
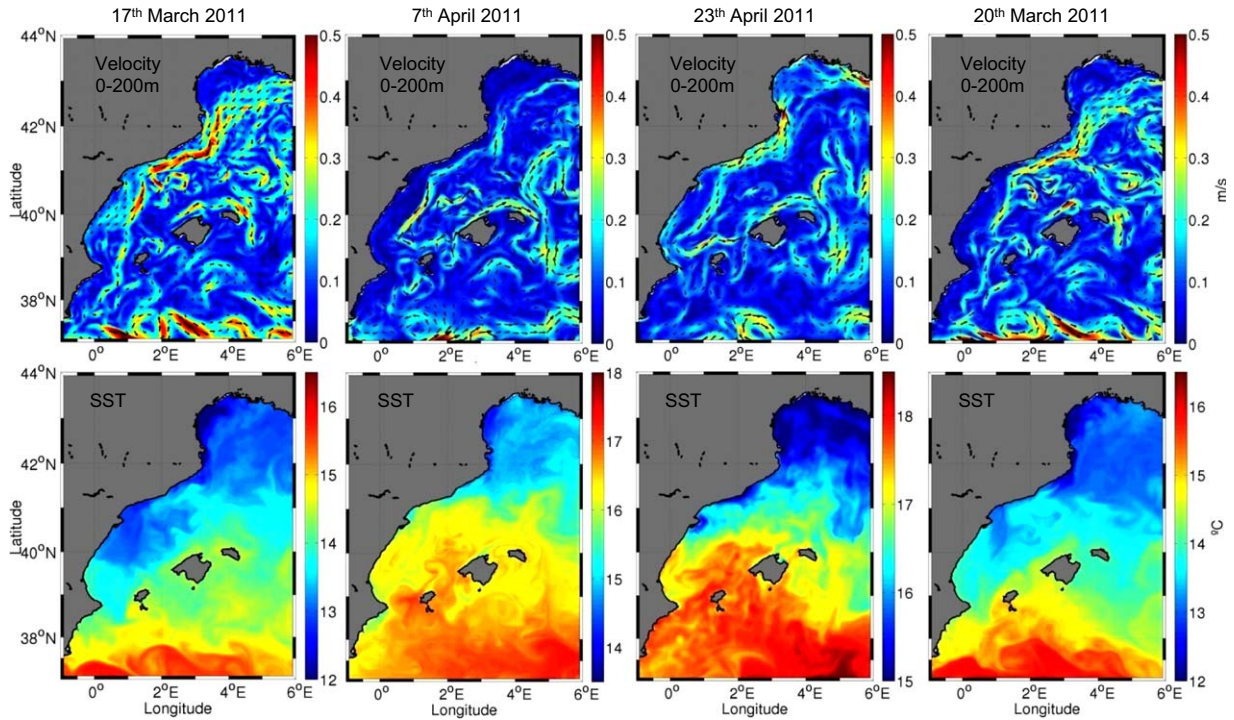
Figure 6. (top) Simulated velocity averaged within the (0–200 m) layer and (bottom) simulated Sea Surface Temperature on the 17 March 2011, the 7 April 2011, the 23 April 2011, and the 20 March 2011 (from left to right).

4.2. Spatial and Temporal Variability

[19] The spatial and temporal variability of the WIW in the NWMED is studied analyzing the transport of WIW in key sections across the sites of formation and the main pathways (see Figure 1b) in the full simulation from 15 February to 30 June 2011 (Figures 8a–8d). The maxima of WIW transports in every section are reported in Figure 8e. In the Gulf of Lion, the simulated WIW is mainly formed along the continental shelf between mid-February and mid-

March 2011 and circulates southwestward (Figures 8a and 8e). The maximum of WIW outflow transport is reached the 1 March: 0.23 Sv, 0.38 Sv, 0.81 Sv through *GoLA*, *GoLB*, *GolC*, respectively. Although the Northern Current flowing through *GoLA* is induced and influenced by the Mercator PSY2V4R3 simulation at the eastern boundary, no WIW was formed or present upstream of the transect *GoLA*, insuring that the WIW present in the sections *GoLA*, *GoLB*, and *GolC* are formed in the Gulf of Lion region in
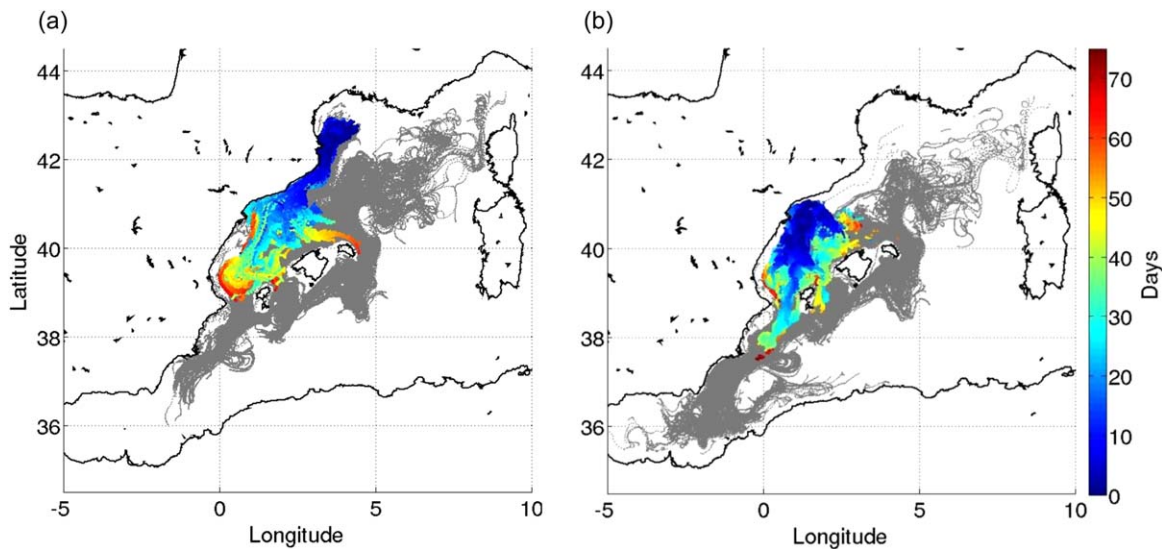

Figure 7. Same as Figure 5 with all trajectories shown. Color indicates time for particles with WIW properties; when WIW properties are lost, trajectories are indicated in gray.
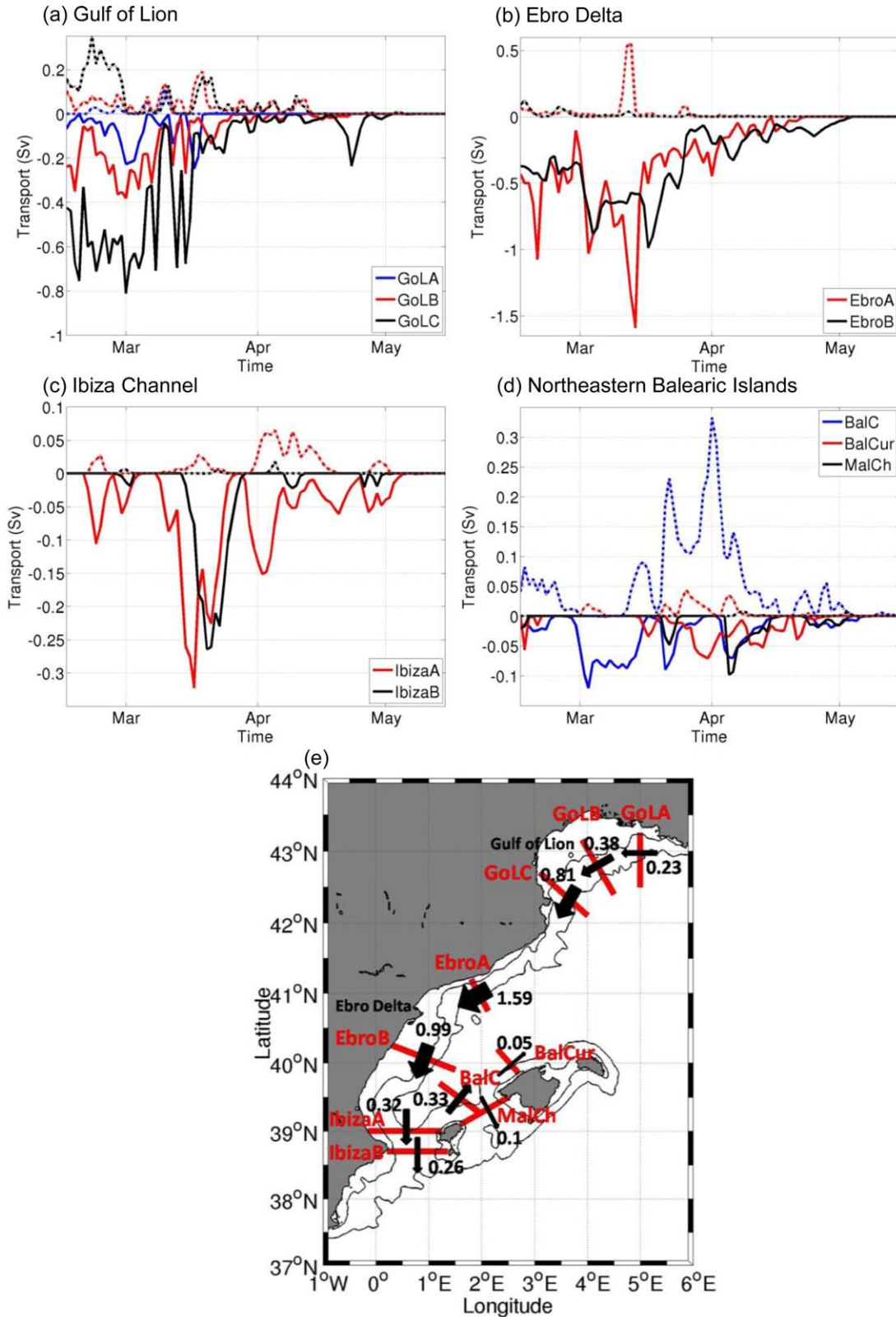
Figure 8. Inflow (dashed lines) and outflow (solid lines) transports (in Sv) of simulated WIW in the ten sections, indicated in Figure 1b (a–d). Scheme of the WIW transports maxima (in Sv) in every section (e).

our case study. Note that the inflow transport is not equal to zero in *GoLB* and *GolC* but weaker than the outflow transport; it indicates that a few WIW particles formed in the

Gulf of Lion recirculate in the continental plateau before losing their properties. In the Ebro Delta region, WIW is present from February to April; the maximum of WIW
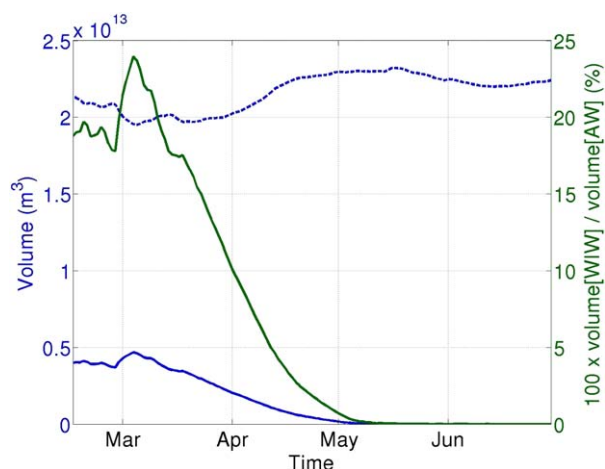
Figure 9. Volumes of simulated AW and WIW (dashed and solid blue lines, respectively), and the percentage of the WIW volume in comparison with the AW volume (green line) as a function of time in the NWMED (0.5°W–5°E, 38°N–44°N).

outflow transport reaches 1.59 Sv/0.99 Sv through *EbroA*/*EbroB* in mid-March (the 14 and 17, respectively, Figures 8b and 8e). The transport in *EbroA* is higher than in the Gulf of Lion the first two weeks of March, revealing that they combine WIW from the Gulf of Lion and WIW formed along the Catalan coast. Interestingly, the transport in *EbroA* is of the same order of magnitude or higher (in mid-March) than in *EbroB*. In fact, a part of the WIW near the Ebro Delta bifurcates eastward (Figure 5) and is partially compensated by the WIW formation between *EbroA* and *EbroB*. In the Ibiza Channel region (Figures 8c and 8e), in good agreement with *Heslop et al.* [2012], the simulated WIW is present from February to May with a maximum of the outflow transport in mid-to-late March (0.32 Sv in *IbizaA*, 0.26 Sv in *IbizaB*). Note the transport through *IbizaA* and *IbizaB* are somewhat different. Before mid-March and after late-March, there is no transport through *IbizaB* indicating that the WIW recirculates northeastward to join the BC. In mid-to-late March, the WIW (up to 0.26 Sv) goes southward through the Ibiza Channel with maximum transport the 20 March 2011. Most of WIW recirculating northeastward joins the BC, where WIW inflow transport is up to 0.1 Sv from mid-March to early-April with a maximum of 0.33 Sv the 1 April (see *BalC* in Figures 8d and 8e). The WIW transports in *IbizaB* and *BalC* represent at most 25% and 30%, respectively, of the transport through *EbroB*, and the inflow transport in *BalCur* is weaker (less than 0.05 Sv) than in *BalC*: this indicates that most of WIW lose their T/S properties (by dilution with surrounding waters) in the southern part of the Balearic Sea. Finally, consistently with *Pinot and Ganachaud* [1999] and *Pinot et al.* [2002], the Ibiza Channel is likely the favorite pathway of WIW to the south, since the WIW transport through the Mallorca Channel (*MalCh* in Figures 8d and 8e) is weaker (maximum of 0.1 Sv versus 0.26 Sv) and occurs during a very short period in early-April.

[20] The results emerging from the WIW transports and Lagrangian trajectories (schematized in Figures 5e and 8e, respectively) are complementary and lead to the conclusion

that during the winter-spring 2011, WIW is mainly formed in the western Gulf of Lion and the Ebro Delta region in February–March, circulates southward joining the northeastern Balearic Sea, or going further south and joining the Balearic Current, or going through the Ibiza and Mallorca Channels. Additionally, as depicted in Figure 9, during the late-winter/early-spring 2011, the presence of WIW in the NWMED is quantitatively significant. Indeed, the WIW volume over the NWMED represents more than 20% of the AW volume between the 28 February and the 11 March 2011, reaching its maximum of 24% 4 March, supporting the importance of WIW in the NWMED.

4.3. Vertical Structure

[21] In order to determine the vertical structure of the main pathways of WIW, vertical sections of temperature (T), salinity (S), and normal velocity to the section (V) are done in the sections *GoLC*, *EbroB*, *IbizaB*, *BalC*, and *MalCh* at the date associated to the maximal transport of WIW (Figure 8), i.e., the 1 March, 17 March, 20 March, 1 April, and 5 April, respectively (Figure 10). In the section *GoLC* (Figure 10a), the WIW occupies the upper 200 m layer on the continental shelf (since it is formed in this coastal area by surface cooling of AW) and flows southward with a velocity of 0.1–0.2 m/s. Deeper, along the continental shelf, LIW spreads southward at 0.3–0.4 m/s with T and S maxima at 400–500 m depth. In the section *EbroB* (Figure 10b), the WIW circulates southward over the continental plateau (shallower than 100 m) and along the continental shelf (until 1.3°E) in the upper 250 m with a normal velocity of 0.2 m/s. It lies above a deep LIW spreading faster southward with a core depth of 300–400 m (where T and S maxima are found). As the WIW, the maximal velocity of LIW (up to 0.3 m/s) is also reached along the continental slope. In the section *IbizaB* (Figure 10c), the WIW goes across the Ibiza Channel southward in its central part between 0.55°E and 0.9°E at 50–150 m depth. The maximum of its velocity reaches 0.17 m/s at 0.7°E. The WIW core flows to the south beneath the surface AW and above the LIW core, which also flows southward at 0.1–0.2 m/s. Further east, between 0.8°E and 1.1°E, AW flows along the slope northward through the Ibiza Channel with a velocity of 0.1 m/s at 100–500 m depth. At the eastern part of the Ibiza Channel, in the upper 100 m, recent AW (warmer than Mediterranean Waters in winter and fresh) is spreading northward through the channel with a velocity of around 0.1 m/s. In the section *BalC* (Figure 10d), the WIW circulates northeastward at 50–200 m, above LIW (with a core depth at 500 m) and deep water in the deeper layer, between 39.37°N and 39.68°N with a weak velocity (less than 0.1 m/s). The maximum of velocity (0.25 m/s) is found between 1.6°E and 1.9°E at 400–700 m depth in the northeastward direction. Finally, in the section *MalCh* (Figure 10e), the second pathway to the southern Mediterranean Sea, the WIW flows out of the Balearic Sea through the Mallorca Channel at 100–200 m depth, beneath the surface AW and above the LIW. The maximal velocity of WIW is up to 0.1 m/s in the center part of the channel (1.9°E) at 150 m depth. In the western part of the channel (1.6°E–1.8°E), AW flows northward, and in a similar manner as in the Ibiza Channel, recent AW enters in the Balearic Sea through the eastern part of the Mallorca Channel.
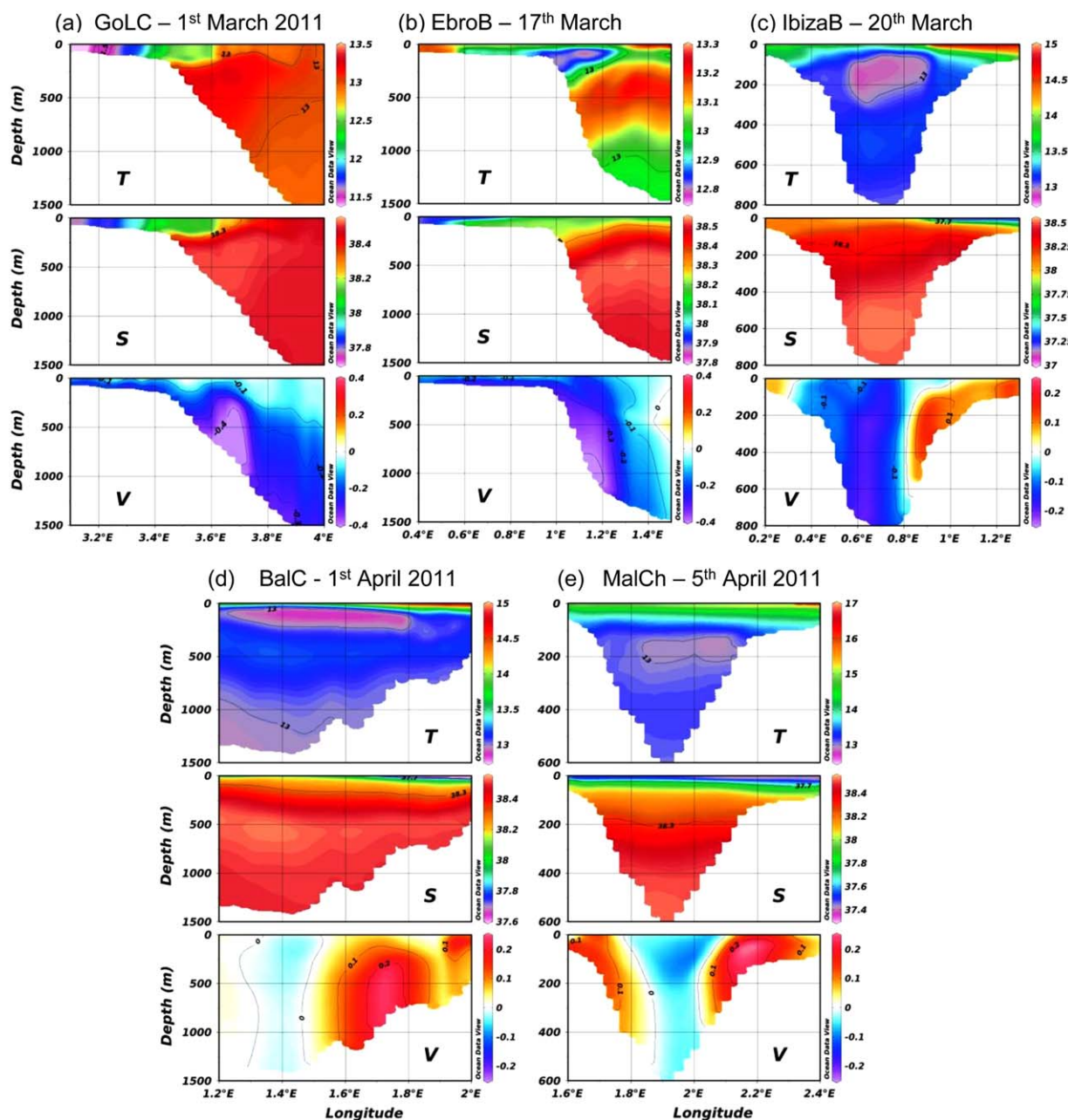
Figure 10. Vertical sections of simulated temperature, salinity, and normal velocity to the section in five transects: (a) *GoLC* on the 1 March, (b) *EbroB* on the 17 March, (c) *IbizaB* on the 20 March, (d) *BalC* on the 1 April, and (e) *MalCh* on the 5 April. Note that positive (negative) velocity signs indicate northward/eastward (southward/westward) direction.

5. Conclusions

[22] In this study, the formation, spreading, and main pathways of the WIW in the Northwestern Mediterranean Sea have been examined combining available observations and numerical simulation during the winter-spring 2011. The main results show that the simulation is able to reproduce the WIW formation and the main characteristics of the water masses present during the studied period. Lagrangian particles and transports through key sections in the simulation indicate that WIW is formed mainly in the Gulf of Lion and the Ebro Delta region in February–March and

then, circulates southward following five main trajectories: WIW joins the Northeastern Balearic Sea (P_G^1, P_E^1), recirculates cyclonically reaching the Balearic Current (P_G^2, P_E^3) with a maximum transport of 0.33 Sv in early-April, circulates southward until the Ibiza Channel (P_G^3, P_E^4), goes through the Ibiza Channel (P_E^2) or the Mallorca Channel (P_E^5) with a maximum of 0.26 Sv in late-March or 0.1 Sv in early-April, respectively. WIW contributes notably to the exchanges of mass and heat between the north and south basins of the Western Mediterranean Sea [*Allen et al.*, 2008] and therefore, those five pathways of WIW reported

in this work represent a significant improvement for the knowledge of the WIW circulation variability in the Western Mediterranean Sea. Indeed, we have shown that WIW formed in the Gulf of Lion and the Ebro Delta region may likely have an impact on the general circulation of the Western Mediterranean Sea reaching areas such as the Algero-Provencal and Alboran basins.

[23] Despite some simulation biases, a good agreement has been found between water masses from the simulation and high resolution hydrographic glider observations, in particular, in the Ibiza Channel which seems to be the preferred path of WIW to flow out of the Balearic Sea to the south. Some discrepancies found in water masses and derived variables might be due to several modeling factors (atmospheric forcing, initial conditions, parameterizations, climatological run off, etc.) and may influence the results (WIW formation, pathways, transport estimations). However, the realism of the simulation and its capacity to reproduce observed water masses is encouraging and argues in favor of (i) investigating ocean processes study (formation, transformation and mixing of water masses, in particular WIW and WMDW, and their dynamical impact on the ocean stratification and circulation) and (ii) developing a long-term high-resolution oceanic simulation to assess the variability of WIW (and other water masses) and its impact on the circulation at various timescales.

[24] Finally, this approach could be applied to other parts of the Mediterranean Sea to investigate the pathways of WIW formed in other sites (Ligurian Sea, Western Tyrrhenian Sea) and also of other water masses formed in the Mediterranean Sea.

References

Allen, J. T., S. C. Painter, and M. Rixen (2008), Eddy transport of Western Mediterranean Intermediate Water to the Alboran Sea, *J. Geophys. Res.*, *113*, C04024, doi:10.1029/2007JC004649.

Amores, A., S. Montserrat, and M. Marcos (2013), Vertical structure and temporal evolution of an anticyclonic eddy in the Balearic Sea (western Mediterranean), *J. Geophys. Res.*, *118*(4), 2097–2106, doi:10.1002/jgrc.20150.

Astraldi, M., S. Balopoulos, J. Candela, J. Font, M. Gacic, G. P. Gasparini, B. Manca, A. Theocharis, and J. Tintoré (1999), The role of straits and channels in understanding the characteristics of Mediterranean circulation, *Prog. Oceanogr.*, *44*, 65–108.

Ben Ismail, S., C. Sammari, G. P. Gasparini, K. Béranger, M. Brahim, and L. Aleya (2012), Water masses exchanged through the Channel of Sicily: Evidence for the presence of new water masses on the Tunisian side of the Channel, *Deep Sea Res., Part I*, *63*, 65–81, doi:10.1016/j.dsr.2011.12.009.

Béthoux, J.-P. (1980), Mean water fluxes across sections in the Mediterranean Sea, evaluated on the basis of water and salt budget and of observed salinities, *Oceanol. Acta*, *3*, 79–88.

Bouffard, J., A. Pascual, S. Ruiz, Y. Faugre, and J. Tintoré (2010), Coastal and mesoscale dynamics characterization using altimetry and gliders: A

case study in the Balearic Sea, *J. Geophys. Res.*, *115*, C10029, doi:10.1029/2009JC006087.

Bouffard, J., L. Renault, S. Ruiz, A. Pascual, C. Dufau, and J. Tintoré (2012), Sub-surface small-scale eddy dynamics from multi-sensor observations and modeling, *Prog. Oceanogr.*, *106*, 62–79.

Dufau-Julliand, C., P. Marsaleix, A. Petrenko, and I. Dekeyser (2004), Three-dimensional modeling of the Gulf of Lion's hydrodynamics (northwest Mediterranean) during January 1999 (MOOGLI3 Experiment) and late winter 1999: Western Mediterranean Intermediate Water's (WIW) formation and its cascading over the shelf break, *J. Geophys. Res.*, *109*, C11002, doi:10.1029/2003JC002019.

Estournel, C., X. Durrieu de Madron, P. Marsaleix, F. Auclair, C. Julliand, and R. Vehil (2003), Observation and modeling of the winter coastal oceanic circulation in the Gulf of Lion under wind conditions influenced by the continental orography (FETCH experiment), *J. Geophys. Res.*, *108*(C3), 8059, doi:10.1029/2001JC000825.

Fairall, C. F., E. F. Bradley, J. E. Hare, A. A. Grachev, and J. B. Edson (2003), Bulk parameterization of air-sea fluxes: Updates and verification for the COARE algorithm, *J. Clim.*, *16*, 571–591, doi:10.1175/1520-0442(2003)016 <0571:BPOASF >2.0.CO;2.

Flamant, C. (2003), Alpine lee cyclogenesis influence on air-sea heat exchanges and marine atmospheric boundary layer thermodynamics over the western Mediterranean during a Tramontane/Mistral event, *J. Geophys. Res.*, *108*(C3), 8057, doi:10.1029/2001JC001040.

Font, J. (1990), A comparison of seasonal winds with currents on the continental slope of the Catalan Sea (northwestern Mediterranean), *J. Geophys. Res.*, *95*(C2), 1537–1545.

Font, J., J. Salat, and J. Tintoré (1988), Permanent features of the circulation in the Catalan Sea, in *Pelagic Mediterranean Oceanogr.*, edited by H. J. Minas and P. Nival, Oceanologica Acta, vol. *9*, 51–57.

Fuda, J. L., C. Millot, I. Taupier-Letage, U. Send, and J. M. Bocognano (2000), XBT monitoring of a meridian section across the western Mediterranean Sea, *Deep Sea Res.*, Part I, *47*(11), 2191–2218.

Garau, B., S. Ruiz, W. G. Zhang, A. Pascual, E. Heslop, J. Kerfoot, and J. Tintoré (2011), Thermal lag correction on Slocum CTD glider data, *J. Atmos. Ocean. Technol.*, *28*(9), 1065–1071, doi:10.1175/JTECH-D-10-05030.1.

Gasparini, G. P., G. Zodiatis, M. Astraldi, C. Galli, and S. Sparnochia (1999), Winter intermediate water lenses in the Ligurian Sea, *J. Mar. Syst.*, *20*, 319–332.

Gasparini, G. P., A. Ortona, G. Budillon, M. Astraldi, and E. Sansone (2005), The effect of the Eastern Mediterranean Transient on the hydrographic characteristics in the Strait of Sicily and in the Tyrrhenian Sea, *Deep Sea Res., Part I*, *52*, 915–935, doi:10.1016/j.dsr.2005.01.001.

Hamming, R. W. (1959), Stable predictor-corrector methods for ordinary differential equations, *J. Assoc. Comput. Mach.*, *6*, 37–47.

Herrmann, M., F. Sevault, J. Beuvier, and S. Somot (2010), What induced the exceptional 2005 convection event in the northwestern Mediterranean basin? Answer from a modeling study, *J. Geophys. Res.*, *115*, C12051, doi:10.1029/2010JC006162.

Heslop, E., S. Ruiz, J. Allen, J. L. López-Jurado, L. Renault, and J. Tintoré (2012), Autonomous underwater gliders monitoring variability at "choke points" in our ocean system: A case study in the Western Mediterranean Sea, Geophys. *Res. Lett.*, *39*, L20604, doi:10.1029/2012GL053717.

Ingleby, B., and M. Huddleston (2007), Quality control of ocean temperature and salinity profiles—Historical and real-time data, *J. Mar. Syst.*, *65*, 158–175, doi:10.1016/j.jmarsys.2005.11.019.

Jansá, A. (1987), Distribution of the mistral: A satellite observation, *Meteorol. Atmos. Phys.*, *36*, 201–214.

La Violette, P. E. (1994), *Overview of the major forcings and water masses of the Western Mediterranean Sea, in Seasonal and Inter annual variability of the Western Mediterranean Sea*, edited by P. E. La Viollette, vol. *46*, pp. 1–11, AGU, Washington, D. C.

La Violette, P. E., J. Tintoré, and J. Font (1990), The surface circulation of the Balearic Sea, *J. Geophys. Res.*, *95*, 1559–1568.

Lellouche, J.-M., et al. (2013), Evaluation of global monitoring and forecasting systems at Mercator Océan, *Ocean Sci.*, *9*, 57–81, doi:10.5194/os-9-57-2013.

López-Jurado, J. L., J. Garciá Lafuente, and N. Cano Lucaya (1995), Hydrographic conditions of the Ibiza Channel during November 1990, March 1991 and July 1992, Oceanol. Acta, *18*, 235–243.

Marchesiello, P., J. C. McWilliams, and A. Shchepetkin (2001), Open boundary conditions for long-term integration of regional oceanic models, *Ocean Modell.*, *3*, 1–20, doi:10.1016/S1463–5003(00)00013-5.

Mertens, C., and F. Schott (1998), Interannual variability of deep-water formation in the Northwestern Mediterranean, *J. Phys. Oceanogr.*, *28*, 1410–1424.

Millot, C. (1999), Circulation in the Western Mediterranean Sea, *J. Mar. Syst.*, *20*, 423–442.

Millot, C. (2009), Another description of the Mediterranean Sea outflow, *Prog. Oceanogr.*, *82*, 101–124, doi:10.1016/j.pocean.2009.04.016.

Millot, C. (2013), Levantine intermediate water characteristics: An astounding general misunderstanding!, *Sci. Mar.*, *77*(2), 217–232, doi:10.3989/scimar.03518.13A.

Millot, C., and I. Taupier-Letage (2005), Circulation in the Mediterranean Sea, *in The Mediterranean Sea*, pp. 29–66, Springer, Berlin Heidelberg.

Monserrat, S., J. L. López-Jurado, and M. Marcos (2008), A mesoscale index to describe the regional circulation around the Balearic Islands, *J. Mar. Syst.*, *71*, 413–420.

Pinot, J.-M., J. Tintoré, and D. Gomis (1995), Multivariate analysis of the surface circulation in the Balearic Sea, *Prog. Oceanogr.*, *36*, 343–376.

Pinot, J.-M., and A. Ganachaud (1999), The role of Winter Intermediate Waters in the spring-summer circulation of the Balearic Sea. Part 1. Hydrography and inverse modelling, *J. Geophys. Res.*, *104*, 29,843–29,864.

Pinot, J.-M., J. L. López-Jurado, and M. Riera (2002), The CANALES experiment (1996–1998). Interannual, seasonal, and mesoscale variability of the circulation in the Balearic Channels, *Prog. Oceanogr.*, *55*, 335–370.

Renault, L., J. Chiggiato, J. C. Warner, M. Gomez, G. Vizoso, and J. Tintoré (2012), Coupled atmosphere-ocean-wave simulations of a storm event over the Gulf of Lion and Balearic Sea, *Geophys. Res. Lett.*, *117*, C09019, doi:10.1029/2012JC007924.

Renault, L., G. Vizoso, A. Jansá, J. Wilkin, and J. Tintoré (2011), Toward the predictability of meteotsunamis in the Balearic Sea using regional nested atmosphere and ocean models, *Geophys. Res. Lett.*, *38*, L10601, doi:10.1029/2011GL047361.

Robinson, A. R., W. G. Leslie, A. Theocharis, and A. Lascaratos (2001), *Encyclopedia of Ocean Sciences*, vol. *3*, chap. Mediterranean Sea Circulation, pp. 1689–1705, Academic, London, doi:10.1006/rwos.2001.0376.

Ruiz, S., L. Renault, B. Garau, and J. Tintoré (2012), Underwater glider observations and modeling of an abrupt mixing event in the upper ocean, *Geophys. Res. Lett.*, *39*, L01603, doi:10.1029/2011GL050078.

Salat, J., and J. Font (1987), Water mass structure near and offshore the Catalan coast during the winter of 1982 and 1983, *Ann. Geophys.*, *5*, 49–54.

Salat, J., P. Puig, and M. Latasa (2010), Violent storms within the Sea: Dense water formation episodes in the NW Mediterranean, *Adv. Geosci.*, *26*, 53–59, doi:10.5194/adgeo-26-53-2010.

Schroeder, K., A. Ribotti, M. Borghini, R. Sorgente, A. Perilli, and G. P. Gasparini (2008), An extensive western Mediterranean deep water renewal between 2004 and 2006, *Geophys. Res. Lett.*, *35*, L18605, doi:10.1029/2008GL035146.

Send, U., J. Font, G. Krahmann, C. Millot, M. Rhein, and J. Tintoré (1999), Recent advances in observing the physical oceanography of the western Mediterranean Sea, *Prog. Oceanogr.*, *44*, 37–64.

Shchepetkin, A. F., and J. C. McWilliams (2005), The regional oceanic modeling system (ROMS): A split explicit, free-surface, topography-following-coordinate oceanic model, *Ocean Modell.*, *9*, 347–404, doi:10.1016/j.ocemod.2004.08.002.

Skamarock, W. C., J. B. Klemp, J. Dudhia, D. O. Gill, D. M. Barker, M. Duda, X. Y. Huang, W. Wang, and J. G. Powers (2008), A description of the advanced research WRF version 3, NCAR Tech. Note NCAR/TN–475+STR, Natl. *Cent. for Atmos. Res., Boulder, Colo*.

Smith, W. H. F., and D. T. Sandwell (1997), Global sea floor topography from satellite altimetry and ship depth soundings, *Science*, *277*, 1956–1962, doi:10.1126/science.277.5334.1956.

Sparnocchia, S., P. Picco, G. M. R. Manzella, A. Ribotti, S. Copello, and P. Brasey (1995), Intermediate water formation in the Ligurian Sea, *Oceanol. Acta*, *18*, 151–162.

Tintoré, J., et al. (2013), SOCIB: The Balearic Islands coastal ocean observing and forecasting system responding to science, technology and society needs, *Mar. Technol. Soc. J.*, *47*(1), 101–117.

Vargas-Yáñez, M., P. Zunino, K. Schreder, J. L. López-Jurado, F. Plaza, M. Serra, C. Castro, M. C. Garca-Martnez, F. Moya, and J. Salat (2012), Extreme Western Intermediate Water formation in winter 2010, *J. Mar. Syst.*, *105–108*, 52–59, doi:10.1016/j.jmarsys.2012.05.010.